This article was downloaded by: [Renmin University of China]
On: 13 October 2013, At: 10:33
Publisher: Taylor & Francis
Informa Ltd Registered in England and Wales Registered Number: 1072954 Registered office: Mortimer House, 37-41 Mortimer Street, London W1T 3JH, UK

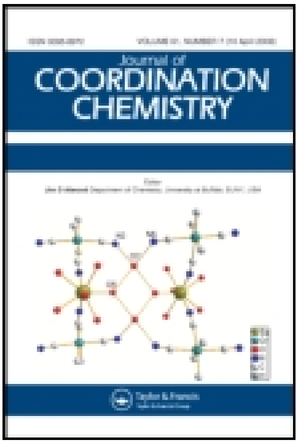

Journal of Coordination Chemistry
Publication details, including instructions for authors and subscription information:
http://www.tandfonline.com/loi/gcoo20

The first in situ tetrazole synthesis of lanthanide metal coordination frameworks

Jun Wang [a], Jianhua Nie [a] & Chuntao Dai [a]

[a] Department of Chemical Engineering, Zhongshan Polytechnic, Zhongshan, Guangdong 528404, P.R. China

Published online: 09 May 2011.

To cite this article: Jun Wang, Jianhua Nie & Chuntao Dai (2011) The first in situ tetrazole synthesis of lanthanide metal coordination frameworks, Journal of Coordination Chemistry, 64:9, 1645-1653, DOI: 10.1080/00958972.2011.578626

To link to this article: http://dx.doi.org/10.1080/00958972.2011.578626

PLEASE SCROLL DOWN FOR ARTICLE

Taylor & Francis makes every effort to ensure the accuracy of all the information (the “Content”) contained in the publications on our platform. However, Taylor & Francis, our agents, and our licensors make no representations or warranties whatsoever as to the accuracy, completeness, or suitability for any purpose of the Content. Any opinions and views expressed in this publication are the opinions and views of the authors, and are not the views of or endorsed by Taylor & Francis. The accuracy of the Content should not be relied upon and should be independently verified with primary sources of information. Taylor and Francis shall not be liable for any losses, actions, claims, proceedings, demands, costs, expenses, damages, and other liabilities whatsoever or howsoever caused arising directly or indirectly in connection with, in relation to or arising out of the use of the Content.

This article may be used for research, teaching, and private study purposes. Any substantial or systematic reproduction, redistribution, reselling, loan, sub-licensing, systematic supply, or distribution in any form to anyone is expressly forbidden. Terms & Conditions of access and use can be found at http://www.tandfonline.com/page/terms-and-conditions

Journal of Coordination Chemistry
Vol. 64, No. 9, 10 May 2011, 1645–1653

The first *in situ* tetrazole synthesis of lanthanide metal coordination frameworks

JUN WANG, JIANHUA NIE and CHUNTAO DAI*

Department of Chemical Engineering, Zhongshan Polytechnic, Zhongshan, Guangdong 528404, P.R. China

(*Received 5 January 2011; in final form 16 March 2011*)

Hydrothermal reaction of 4-cyanobenzoic acid with NaN_3 in the presence of $Ln(NO_3)_3 \cdot 6H_2O$ produced two lanthanide complexes, $[LnL(HL)(H_2O)_5]$ [Ln = Eu (**1**) and Tb (**2**)] (H_2L = 4-(1*H*-tetrazol-5-yl)benzoic acid). Both compounds were structurally characterized by elemental analysis, IR spectroscopy, and single-crystal X-ray diffraction. Complexes **1** and **2** are isostructural and display 3-D supramolecular frameworks. Solid-state properties such as thermal behaviors and photoluminescence for these crystalline materials were also investigated.

Keywords: *In situ* tetrazole ligand synthesis; Crystal structure; Lanthanide metal; Photoluminescence

1. Introduction

Design and synthesis of tetrazole-based coordination compounds have gained interest due to their intriguing topological structures and their potential applications as advanced materials [1]. A number of 5-substituted tetrazole-based complexes have been reported, including 5-methyl-, 5-ethyl-, 5-propyl-, 5-amino-, 5-pyrazinyl-, 5-(2-pyridyl)-, 5-(3-pyridyl)-, 5-(4-pyridyl)-, 1,5-diaminotetrazole, 1,4-benzeneditetrazolate, 1,3,5-benzenetristetrazolate, etc. [2–16]. For instance, Xiong *et al*. prepared myriad interesting metal–organic coordination polymers that not only partially showed the role of the metal species in the synthesis of tetrazole compounds but also provided a class of complexes displaying interesting chemical and physical properties such as second harmonic generation (SHG), fluorescence, ferroelectric, and dielectric behaviors [1]; Bu *et al*. synthesized a pcu-type topological network constructed by DTA^{2-} (DTA^{2-} = 9,10-ditetrazolateanthracene) bridging rare heptanuclear $[Zn_7(OH)_8]^{6+}$ clusters [12]; Qiu *et al*. reported a high-symmetry cubic coordination framework exhibiting reversible shrinkage and expansion in a crystal-to-crystal dehydration/rehydration process [13].

Since Sharpless and co-workers described a safe, convenient, and environment-friendly route to synthesize 5-substituted 1*H*-tetrazole complexes through [2 + 3] cycloaddition reactions of nitriles and azide in the presence of zinc salt as Lewis acid

---

*Corresponding author. Email: daicuntao@126.com

Journal of Coordination Chemistry
ISSN 0095-8972 print/ISSN 1029-0389 online
DOI: 10.1080/00958972.2011.578626

[17–19], this synthetic approach has been extended to various metal ions such as Zn^{II}, Cd^{II}, Cu^{I}/Cu^{II}, Fe^{II}, Co^{II}, Mn^{II}, and Ag^{I} in the construction of coordination frameworks [1–19]. Among these complexes, the role of these transition metals is still unclear; in particular, studies on lanthanide coordination polymers through *in situ* tetrazole ligand synthesis are still rare, allowing us to further explore the coordination chemistry of tetrazoles.

In this study, we design a carboxylate-tetrazole ligand through *in situ* tetrazole formation with lanthanide as a catalyst, 4-(1*H*-tetrazol-5-yl)benzoic acid (H_2L), to construct lanthanide-based coordination compounds, based on several considerations: (1) 4-(1*H*-tetrazol-5-yl)benzoic acid possessing both carboxylate and tetrazole ring is expected to exhibit various coordinating modes in the construction of multidimensional coordination frameworks; (2) tetrazole with four nitrogen H-bonding acceptors is able to form H-bonding in the growth of single crystal; (3) lanthanide not only has various coordination numbers, but also shows luminescence when coordinated to functional ligands [20–24]; (iv) lanthanide coordination complexes through *in situ* tetrazole formation have not been reported before.

By hydrothermally treating 4-cyanobenzoic acid with NaN_3 in the presence of $Ln(NO_3)_3 \cdot 6H_2O$, we obtained $[LnL(HL)(H_2O)_5]$ [Ln = Eu (**1**) and Tb (**2**)] (H_2L = 4-(1*H*-tetrazol-5-yl)benzoic acid), and their structures have been determined by elemental analysis, IR spectroscopy, and single-crystal X-ray diffraction. In addition, thermal stability and solid-state fluorescent properties of the two coordination polymers have also been explored.

2. Experimental

2.1. *Materials and instruments*

All materials and reagents were obtained commercially and used without purification. Elemental (C, H, and N) analyses were performed on a Perkin Elmer 2400 element analyzer. Infrared samples were prepared as KBr pellets and spectra obtained from 4000 to 400 cm^{-1} using a Nicolet Avatar 360 FT-IR spectrophotometer. Thermogravimetric analysis (TGA) experiments were carried out on a Perkin Elmer TGA 7 thermogravimetric analyzer with a heating rate of 10°C min^{-1} from 35 to 750°C under dry air. Fluorescence spectra were recorded with an Edinburgh FLS920 Spectrophotometer analyzer.

2.2. *Synthesis of 1 and 2*

An aqueous mixture (10 mL) of 4-cyanobenzoic acid (0.2 g, 1.36 mmol), $Ln(NO_3)_3 \cdot 6H_2O$ [Ln = Eu, 0.446 g, 1 mmol for **1**; Ln = Tb, 0.453 g, 1 mmol for **2**], and NaN_3 (0.0650 g, 1 mmol) was placed in a 23 mL Teflon-lined stainless-steel autoclave heated to 150°C for 48 h, and then cooled to room temperature at 5°C h^{-1}; colorless block single crystals of **1** (or **2**) were obtained (yield: 38% based on Eu; 41% based on Tb). Elemental analysis Calcd (%) for **1**, $C_{32}H_{38}Eu_2N_{16}O_{18}$: C, 31.03; H, 3.09; and N, 18.09. Found: C, 31.10; H, 2.98; and N, 18.02. IR data (KBr, cm^{-1}): 3454, 1635, 1560, 1500, 1389, 1110, and 1045. Elemental analysis Calcd (%) for **2**,

$C_{32}H_{38}Tb_2N_{16}O_{18}$: C, 30.68; H, 3.06; and N, 17.89. Found: C, 30.75; H, 3.12; and N, 17.82. IR data (KBr, cm^{-1}): 3450, 1634, 1561, 1501, 1385, 1112, and 1045.

2.3. *X-ray crystallography*

Single-crystal X-ray diffraction data collections of **1** and **2** were performed on a Bruker Apex II CCD diffractometer operating at 50 kV and 30 mA using Mo-Kα radiation ($\lambda = 0.71073$ Å). Data collection and reduction were performed using the APEX II software. Multi-scan absorption corrections were applied for all the data sets using the APEX II program [25]. The structures were solved by direct methods and refined by full-matrix least squares on F^2 using the SHELXTL program package [25]. All non-hydrogen atoms were refined with anisotropic displacement parameters. Hydrogens attached to carbon were placed in geometrically idealized positions and refined using a riding model. Hydrogens on water were located from difference Fourier maps and also refined using a riding model.

3. Results and discussion

3.1. *Synthesis and characterization*

The syntheses of **1** and **2** are described in the experimental section. In FT-IR spectra, emergence of peaks in the region 1400–1500 cm^{-1} clearly confirmed the formation of the tetrazole. Features at ~1635 and ~1389 cm^{-1} for **1** and **2** are associated with asymmetric(COO) and symmetric(COO) stretching. A broad band at 3454 and 3450 for **1** and **2**, respectively, may be assigned to ν(O–H) of coordinating water.

Table 1. Crystal data details of the structure determination for **1** and **2**.

Complexes	**1**	**2**
Empirical formula	$C_{32}H_{38}Eu_2N_{16}O_{18}$	$C_{32}H_{38}Tb_2N_{16}O_{18}$
Formula weight	1238.70	1252.62
Temperature (K)	296(2)	296(2)
Crystal system	Triclinic	Triclinic
Space group	$P\bar{1}$	$P\bar{1}$
Unit cell dimensions (Å, °)		
a	8.4111(10)	8.3919(10)
b	10.5483(12)	10.5292(13)
c	13.4198(15)	13.3844(16)
α	110.131(1)	110.170(1)
β	100.670(1)	100.863(1)
γ	101.707(1)	101.648(1)
Volume (Å^3), Z	1051.7(2), 1	1043.5(2), 1
Calculated density ($g\,cm^{-3}$)	1.956	1.993
Absorption coefficient (mm^{-1})	3.051	3.458
$F(000)$	612	616
Goodness-of-fit on F^2	1.051	1.083
R_1 $[I > 2\sigma(I)]^a$	0.0242	0.0244
wR_2 (all data)^b	0.0606	0.0630

$^aR_1 = \sum\|F_o| - |F_c\|/\sum|F_o|$; $^bwR_2 = [\sum_w(F_o^2 - F_c^2)^2/\sum_w(F_o^2)^2]^{1/2}$.

3.2. *Crystal structures of 1 and 2*

X-ray structure analysis reveals that **1** and **2** are isostructural; therefore, **1** is taken as an example to describe in detail (table 1). Complex **1** belongs to triclinic space group $P\bar{1}$ and the asymmetric unit consists of one Eu(III), one 4-(1*H*-tetrazol-5-yl)benzoate monoanion, one 4-(tetrazol-5-yl)benzoate dianion, and five coordinating waters. Each Eu(III) is eight-coordinate with two oxygens from HL, one oxygen from L, and five waters, forming a distorted square-antiprism coordination geometry (figure 1). The Eu–O bond lengths fall in the normal range (table 2) [26, 27]. In **1**, L adopts two kinds of coordination modes (scheme 1 (I and II)). Two neighboring Eu(III) ions are bridged by two bismonodentate carboxylates of two HL; one of the two is coordinated by a monodentate carboxylate of one L and five coordinating waters, leading to the formation of a $Eu_2(L)_2(HL)_2(H_2O)_{10}$ unit. The Eu $\cdots$ Eu separation is *ca* 5.08 Å.

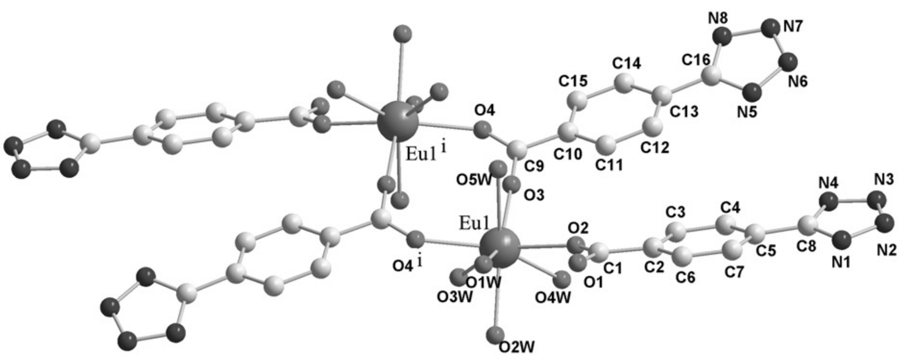

Figure 1. View of an $Eu_2(L)_2(HL)_2(H_2O)_{10}$ unit of **1**. All hydrogens were omitted for clarity. Symmetry code (i): $2-x$, $2-y$, $-z$.

Table 2. Selected bond lengths (Å) and angles (°) for **1** and **2**. Symmetry transformations used to generate equivalent atoms are given as footnotes.

Compound **1**[a]			
Eu1–O3	2.291(3)	Eu1–O4*w*	2.446(3)
Eu1–O2	2.322(2)	Eu1–O5*w*	2.476(3)
Eu1–O4#1	2.346(2)	Eu1–O1*w*	2.481(3)
Eu1–O2*w*	2.410(3)	Eu1–O3*w*	2.482(3)
O3–Eu1–O2	98.47(10)	O3-Eu1–O2*w*	146.54(11)
O2–Eu1–O2*w*	91.05(12)	O3–Eu1–O4*w*	76.44(9)
O4*w*–Eu1–O1*w*	71.61(10)	O5*w*–Eu1–O3*w*	133.41(10)
O4*w*–Eu1–O3*w*	70.93(9)	O4*w*–Eu1–O5*w*	129.54(11)
Compound **2**[b]			
Tb1–O3	2.260(3)	Tb1–O4*w*	2.450(3)
Tb1–O2	2.294(3)	Tb1–O5*w*	2.428(3)
Tb1–O4#1	2.319(3)	Tb1–O1*w*	2.451(3)
Tb1–O2*w*	2.386(3)	Tb1–O3*w*	2.459(3)
O3–Tb1–O2	99.06(11)	O3–Tb1–O5*w*	70.97(13)
O4*w*–Tb1–O3*w*	70.76(10)	O3–Tb1–O2*w*	146.13(12)
O2–Tb1–O4*w*	71.63(10)	O2*w*–Tb1–O5*w*	142.82(12)
O4*w*–Tb1–O1*w*	132.61(10)	O2–Tb1–O5*w*	76.33(11)

[a]#1: $-x+2$, $-y+2$, $-z$; [b]#1: $-x+2$, $-y+2$, $-z$.

Increase in the number of uncoordinated nitrogens within the 5-substituted tetrazole systems results in the broadening of H-bonding types. H-bonding capability of tetrazolic anions with receptor sites is a key for enhanced binding affinity. In the crystal structure packing, the uncoordinated tetrazole moieties are excellent H-bonding

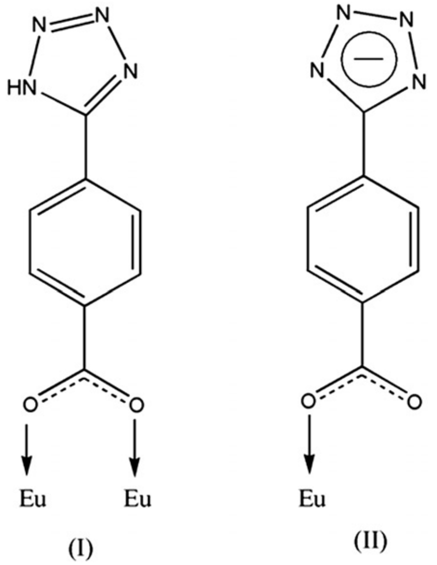

Scheme 1. Coordination modes of *in situ* generation of L.

Table 3. Hydrogen bond lengths (Å) and angles (°) for **1** and **2**.

Donor–H ··· Acceptor	D–H	H ··· A	D ··· A	D–H ··· A
Compound **1**[a]				
O1*w*–H2*w* ··· O1#1	0.84	2.36	3.064(5)	143
O2*w*–H3*w* ··· O1#1	0.83	1.87	2.679(5)	167
O3*w*–H5*w* ··· N3#2	0.83	2.03	2.816(4)	160
O3*w*–H6*w* ··· N6#3	0.83	2.52	3.249(5)	147
O4*w*–H7*w* ··· N4#2	0.83	1.94	2.760(5)	169
N8–H8 ··· N1#4	0.86	2.01	2.833(5)	161
O4*w*–H8*w* ··· N5#2	0.82	2.15	2.912(5)	154
O5*w*–H9*w* ··· N2#5	0.83	2.17	2.965(5)	160
Compound **2**[b]				
O1*w*–H2*w* ··· O1#1	0.84	2.38	3.081(6)	142
O2*w*–H3*w* ··· O1#1	0.84	1.87	2.679(5)	162
O3*w*–H5*w* ··· N3#2	0.82	2.04	2.821(5)	160
O3*w*–H6*w* ··· N6#3	0.83	2.52	3.251(5)	148
O4*w*–H7*w* ··· N4#2	0.83	1.94	2.760(5)	169
N8–H8 ··· N1#4	0.86	2.01	2.842(6)	161
O4*w*–H8*w* ··· N5#2	0.82	2.15	2.915(6)	154
O5*w*–H9*w* ··· N2#5	0.83	2.19	2.965(5)	160
O1*w*–H1*w* ··· N7#6	0.82	2.62	3.291(5)	140

Symmetry transformations used to generate equivalent atoms are given as follows: [a]#1: $1-x$, $1-y$, $-z$; #2: $2-x$, $2-y$, $1-z$; #3: x, $-1+y$, $-1+z$; #4: $1+x$, $1+y$, z; #5: $1-x$, $2-y$, $1-z$.

[b]#1: $1-x$, $1-y$, $-z$; #2: $2-x$, $2-y$, $1-z$; #3: x, $-1+y$, $-1+z$; #4: $1+x$, $1+y$, z; #5:$1-x$, $2-y$, $1-z$; #6: $-1+x$, $-1+y$, $-1+z$.

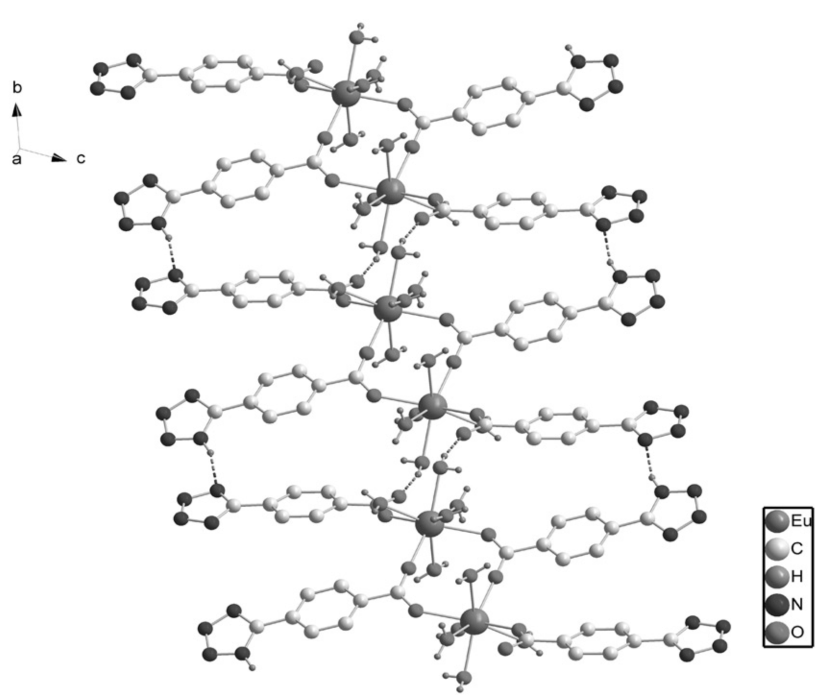

Figure 2. View of a ribbon-like net of **1** linked *via* hydrogen bonds. Hydrogen bonds are shown as dashed lines.

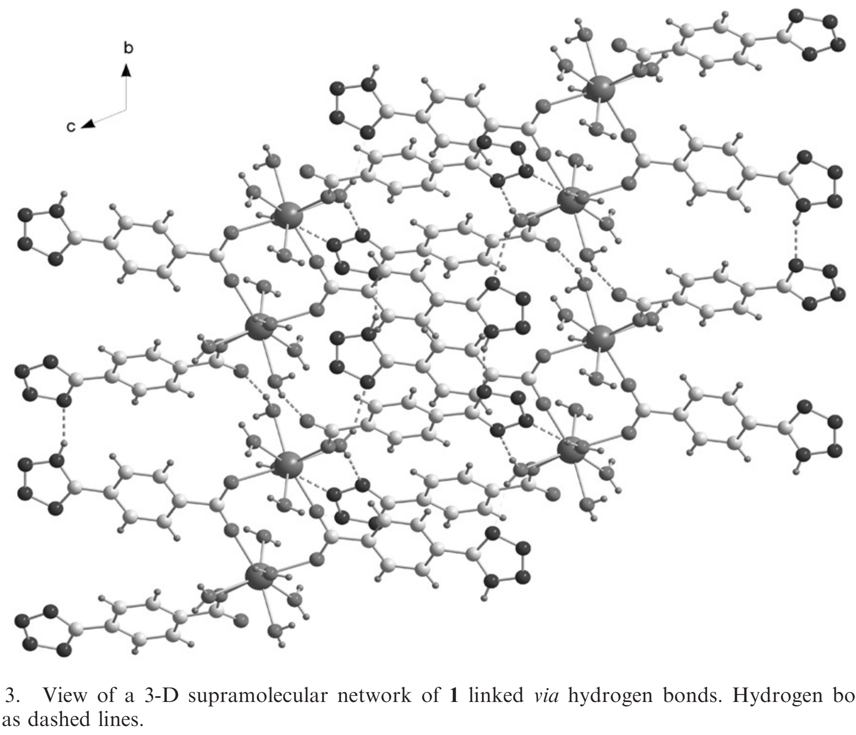

Figure 3. View of a 3-D supramolecular network of **1** linked *via* hydrogen bonds. Hydrogen bonds are shown as dashed lines.

acceptors, while $Ln(H_2O)_5$ units in the middle are H-bonding donors. Additionally, one tetrazole that contains a free N–H bond also has H-bonding donor ability and one monodentate carboxylate is an important H-bonding acceptor. Thus, the $N_{tetrazole}$–$H \cdots N_{tetrazole}$ ($N8 \cdots N1 = 2.833(5)$ Å) and O_{water}–$H \cdots O_{carboxylate}$ interactions ($O2w \cdots O1 = 2.679(5)$ Å) (table 3) assemble neighboring bimetallic units, resulting in the formation of ribbon-like network (figure 2). These nets are further linked by numerous O_{water}–$H \cdots N_{tetrazole}$ ($O \cdots N = 2.8 \sim 3.2$ Å) hydrogen bonding to complete a 3-D supramolecular network (table 3 and figure 3). Weak $\pi \cdots \pi$ stacking contacts between phenyl and tetrazole rings enhance the 3-D network stability.

3.3. *Thermal and luminescent properties*

To study the thermal behaviors of the two complexes, thermogravimetric analyses were done from 35 to 750°C at a heating rate of $10^{\circ}C\,min^{-1}$ in dry air. TGA traces indicated the similarity of the two structures. Waters were eliminated below 150°C, while the removal of organic species took place above 300°C (figure S1).

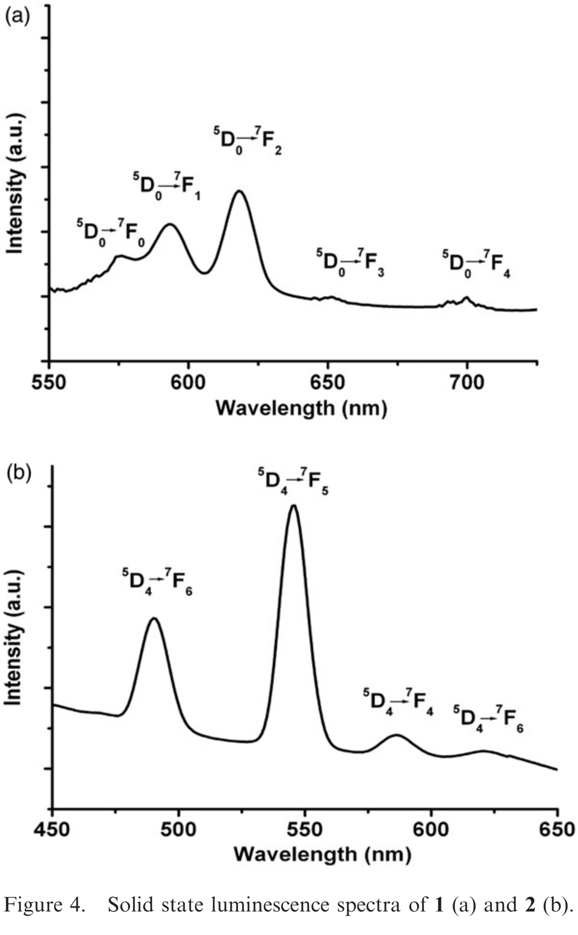

Figure 4. Solid state luminescence spectra of **1** (a) and **2** (b).

Owing to the excellent luminescence of Eu and Tb complexes, luminescence spectra of **1** and **2** were investigated in the solid state when excited by 395 nm for **1** (330 nm for **2**) at room temperature (figure 4). Five typical peaks at 579, 591, 618, 652, and 698 nm, which belong to the characteristic transition of $^5D_0 \rightarrow {}^7F_J$ ($J = 0$–4) of Eu^{3+}, were observed [26–28]. The symmetry-forbidden emission $^5D_0 \rightarrow {}^7F_0$ at 579 nm reveals that Eu^{3+} occupy sites with low symmetry and without an inversion center. The most intense transition is $^5D_0 \rightarrow {}^7F_2$, which implies red emission for **1** (figure 4a). For **2**, the emission spectrum is dominated by the 546 nm peak, suggesting green emission from $^5D_4$-to-$^7F_5$ transition. The other peaks originate from the same excited state, terminating at the ^7F_J manifold (figure 4b).

4. Conclusion

We have prepared two lanthanide tetrazole-based coordination complexes through *in situ* tetrazole synthesis under hydrothermal conditions. Both crystalline materials have high thermal stability and exhibit strong luminescence, with potential applications as photoactive materials. We believe that the synthetic strategies adopted in this study will prevail in the preparation of other lanthanide tetrazole-based coordination networks with interesting structural and functional properties.

Supplementary material

Crystallographic data for the structure reported in this article have been deposited with the Cambridge Crystallographic Data Centre, CCDC no. 805965 & 805966. Copies of this information may be obtained free of charge from the Director, CCDC, 12 Union Road, Cambridge, CB2 1EZ, UK (fax: +44 1223 336 033, e-mail: deposit@ccdc.cam.ac.uk or www: http://www.ccdc.cam.ac.uk), or they are also available from the author on request.

Acknowledgment

This study was supported by Zhongshan Polytechnic.

References

[1] H. Zhao, Z.-R. Qu, H.-Y. Ye, R.-G. Xiong. *Chem. Soc. Rev.*, **37**, 84 (2008).
[2] Y. Tang, Z. Cao, H. Wen, S. Liao, S. Huang, C. Yu. *J. Coord. Chem.*, **63**, 1029 (2010).
[3] G. Xu, T. Hang, K. Pan, Q. Ye. *J. Coord. Chem.*, **62**, 2457 (2009).
[4] X. Zhang, Q. Yu, H. Bian, X. Bao, H. Liang. *J. Coord. Chem.*, **62**, 2108 (2009).
[5] T. Wu, B.-H. Yi, D. Li. *Inorg. Chem.*, **44**, 4130 (2005).
[6] X.-M. Zhang, Y.-F. Zhao, H.-S. Wu, S.R. Batten, S.W. Ng. *Dalton Trans.*, 3170 (2006).
[7] P. Ling, W. Clegg, R.W. Harrington, R.A. Henderson. *Dalton Trans.*, 2388 (2005).

[8] M. Dincă, A. Dailly, Y. Liu, C.M. Brown, D.A. Neumann, J.R. Long. *J. Am. Chem. Soc.*, **128**, 16876 (2006).

[9] M. Dincă, W.S. Han, Y. Liu, A. Dailly, C.M. Brown, J.R. Long. *Angew. Chem., Int. Ed.*, **46**, 1419 (2007).

[10] M. Dincă, J.R. Long. *J. Am. Chem. Soc.*, **129**, 11172 (2007).

[11] S. Horike, M. Dincă, K. Tamaki, J.R. Long. *J. Am. Chem. Soc.*, **130**, 5854 (2008).

[12] J.-R. Li, Y. Tao, Q. Yu, X.-H. Bu. *Chem. Commun.*, 1527 (2007).

[13] H. Deng, Y.C. Qiu, Y.H. Li, Z.H. Liu, R.H. Zeng, M. Zeller, S.R. Batten. *Chem. Commun.*, 2239 (2008).

[14] Y.C. Qiu, H. Deng, S.H. Yang, J.X. Mou, M. Zeller, S.R. Batten, H.H. Wu, J. Li. *Chem. Commun.*, 5415 (2009).

[15] Y.C. Qiu, B. Liu, G. Peng, J.B. Cai, H. Deng, M. Zeller. *Inorg. Chem. Commun.*, **13**, 749 (2010).

[16] Y.C. Qiu, Y.H. Li, G. Peng, J.B. Cai, L.M. Jin, L. Ma, H. Deng, M. Zeller, S.R. Batten. *Cryst. Growth Des.*, **10**, 1332 (2010).

[17] Z.P. Demko, K.B. Sharpless. *J. Org. Chem.*, **66**, 7945 (2001).

[18] Z.P. Demko, K.B. Sharpless. *Org. Lett.*, **3**, 4091 (2001).

[19] Z.P. Demko, K.B. Sharpless. *Angew. Chem., Int. Ed.*, **12**, 2110 (2002).

[20] H. Wang, G. Li, Y. Chen, Z. Zhang, M. Liu. *J. Coord. Chem.*, **63**, 4068 (2010).

[21] L. Dong, Y. Tian, X. Li, Y. Jiang. *J. Coord. Chem.*, **63**, 2088 (2010).

[22] M. Hu, J. Yao, H. Su. *J. Coord. Chem.*, **63**, 1744 (2010).

[23] X. Li, Y. Wang, Z. Ma, R. Zhang, J. Zhao. *J. Coord. Chem.*, **63**, 1029 (2010).

[24] Y. Jiang, X. Wu, X. Li, J. Song, Y. Zou. *J. Coord. Chem.*, **63**, 36 (2010).

[25] Bruker. *APEXII software*, Version 3.1.2; Bruker AXS Inc., Madison, Wisconsin, USA (2004); G.M. Sheldrick. *SHELXL-97, Program for X-ray Crystal Structure Refinement*, University of Göttingen, Göttingen, Germany (1997).

[26] Y. Qiu, H. Liu, Y. Ling, R. Zeng, H. Deng, G. Zhou, M. Zeller. *Inorg. Chem. Commun.*, **10**, 1399 (2007).

[27] Y. Qiu, Z. Liu, J. Mou, H. Deng, M. Zeller. *Cryst. Eng. Comm.*, **12**, 277 (2010).

[28] X. Zhu, S. Gao, Y. Li, H. Yang, G. Li, B. Xu, R. Cao. *J. Solid State Chem.*, **182**, 421 (2009).